Tetrahedron Letters 49 (2008) 5816–5819

Contents lists available at ScienceDirect

Tetrahedron Letters

journal homepage: www.elsevier.com/locate/tetlet

Synthesis and properties of naphthalene trimers linked by 1,3,4-oxadiazole spacers

Katsuhiko Ono [a,*], Hiroki Ito [a], Akihiro Nakashima [a], Mariko Uemoto [a], Masaaki Tomura [b], Katsuhiro Saito [a]

[a] Department of Materials Science and Engineering, Nagoya Institute of Technology, Gokiso, Showa-ku, Nagoya 466-8555, Japan
[b] Institute for Molecular Science, Myodaiji, Okazaki 444-8585, Japan

ARTICLE INFO

Article history:
Received 4 June 2008
Revised 22 July 2008
Accepted 23 July 2008
Available online 26 July 2008

Keywords:
π-Conjugation
Molecular aggregation
Naphthalene
Oxadiazole
Regioisomer

ABSTRACT

Two types of naphthalene trimers linked by 1,3,4-oxadiazole spacers were synthesized and investigated for their physical and electronic properties. 2,6- and 2,7-isomers on central naphthalene moieties were obtained in the forms of pale yellow solids and colorless crystals, respectively. The melting point of the 2,6-isomer was higher than that of the 2,7-isomer. An X-ray crystallographic analysis revealed a π-stacked column with a short intermolecular distance in the crystals of the 2,6-isomer. The absorption maximum of the 2,6-isomer was red-shifted as compared to that of the 2,7-isomer, indicating a π-conjugation between di-2-naphthyloxadiazole moieties in the 2,6-isomer. The quantum yields of the 2,6- and 2,7-isomers were measured to be 0.97 and 0.74, relative to that of 2,5-di-2-naphthyl-1,3,4-oxadiazole (0.85). Molecular orbital (MO) calculations demonstrated that the 2,6-isomer had a higher electron affinity than the 2,7-isomer. Thus, the crosslinking of building blocks is important for the design of functional materials.

1,3,4-Oxadiazole derivatives are highly attractive compounds in the research and development of materials for organic electroluminescent (EL) devices[1] since these compounds possess high electron-accepting properties and exhibit strong fluorescence with high quantum yields. The quantum yields of 2,5-diphenyl-1,3,4-oxadiazole and 2,5-di-2-naphthyl-1,3,4-oxadiazole (**1**) were reported to be 0.80 and 0.85 in cyclohexane solutions, respectively.[2] Thus, compounds involving 1,3,4-oxadiazole rings have been used as electron-transporting materials[1] and emitters[3] in organic EL devices. 2-(4-Biphenylyl)-5-(4-*tert*-butylphenyl)-1,3,4-oxadiazole (PBD) is one of the well-known electron-transporting materials.[4] This π-electron system has been modified to produce spiro-shaped[5] and star-shaped structures,[6] which formed amorphous films with high glass transition temperatures. We synthesized macrocyclic and acyclic bis(2,5-diphenyl-1,3,4-oxadiazole)s (**2** and **3**) and investigated their carrier-transporting properties during the study of organic EL devices.[7] The EL performance of a device using **3** as an electron-transporting layer was considerably higher than that of a device with **2**, although the electronic properties of **2** and **3** were similar to each other. This result was attributed to their molecular structures and aggregations in the solids. Compound **3** had a linear molecular structure and no strong intermolecular interactions were observed in the crystals. The high hole-blocking ability of **3** led to an effective recombination between the holes and electrons at emitting layers. Recently, 1,3,4-oxadiazole dimers linked by aromatic spacers were prepared as linear liquid crystal molecules and a relationship between their thermal properties and molecular structures was reported.[8] With regard to this, we synthesized naphthalene trimers linked by 1,3,4-oxadiazole spacers (**4** and **5**) in order to investigate the properties of linear π-electron systems involving 1,3,4-oxadiazole rings (Fig. 1). The differences between regioisomers **4** and **5** exist in terms of their melting points, absorption and emission maxima, quantum yields, and crystal packings. In this Letter, we report the synthesis, spectral and electrochemical studies, and crystallographic analyses of **4** and **5**.

The synthesis of oxadiazole derivatives **4** and **5** is illustrated in Scheme 1. Naphthalenedicarbohydrazides **7a–b** were obtained by the reactions of dimethyl esters **6a–b** with hydrazine monohydrate.[9] Dicarbohydrazides **7a–b** reacted with 2-naphthoyl chloride in refluxing pyridine to afford compounds **8a–b**[10] that produced **4** and **5** with yields of 39% and 44% by dehydration in refluxing phosphorus(V) oxychloride ($POCl_3$), respectively. These compounds were rarely soluble in common organic solvents although **4** was slightly soluble in chloroform and dichloromethane. Therefore, **4** and **5** were purified by sublimation at 295 and 350 °C under 10^{-3} Torr, respectively. The structure determination of **4** was performed using spectroscopic data and an elemental analysis.[11] The structure of **5** was determined by mass spectrometry, IR, and an elemental analysis.[12]

* Corresponding author. Tel./fax: +81 52 735 5407.
E-mail address: ono.katsuhiko@nitech.ac.jp (K. Ono).

0040-4039/$ - see front matter © 2008 Elsevier Ltd. All rights reserved.
doi:10.1016/j.tetlet.2008.07.122

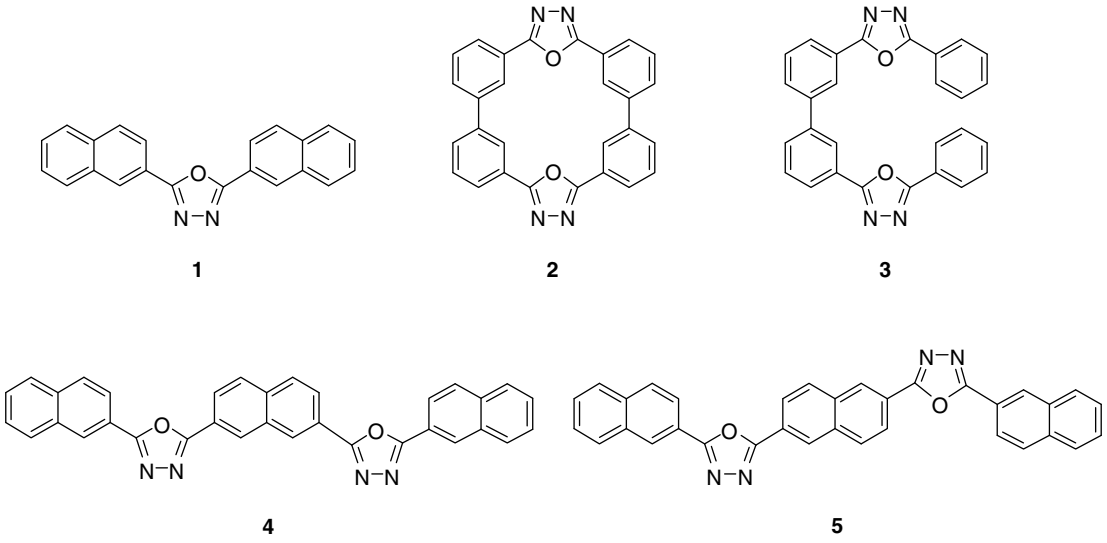

Figure 1. Structure of oxadiazole derivatives **1**–**5**.

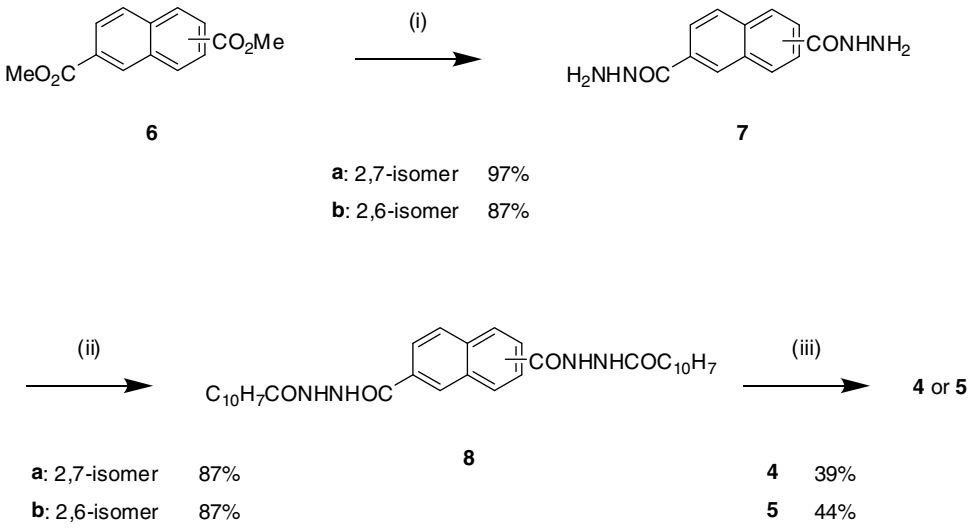

Scheme 1. Synthesis of compounds **4** and **5**. Reagents and conditions: (i) hydrazine monohydrate, $CHCl_3$–MeOH (1:1), reflux; (ii) 2-naphthoyl chloride, pyridine, reflux; (iii) $POCl_3$, reflux.

The melting points, colors, and absorption maxima of **4** and **5** are summarized in Table 1. According to differential scanning calorimetry (DSC) measurements,[13] the melting points of **4** and **5** were considerably higher than the melting point of **1** due to the extension of π-conjugated systems. Further, the melting point of **5** was higher than that of **4**, indicating a dense molecular packing in the crystals of **5**. After melting, the cooling profiles of **4** and **5** exhibited crystallization temperatures of 230.4 and 306.6 °C, respectively. Compounds **4** and **5** were obtained in the forms of colorless crystals and pale yellow solids (Fig. 2). The absorption spectra of **4** and **5** in dichloromethane are presented in Figure 3. The longest absorption maximum of **4** was observed at 341 nm. This value was almost equal to that of **1** (339 nm), suggesting that the extension of a π-electron system in **4** hardly affects the interaction between two di-2-naphthyloxadiazole moieties in terms of the HOMO–LUMO energy gap. Furthermore, the absorption maximum of **5** (361 nm) was red-shifted as compared to the maxima of **4** and **1**, indicating a π-conjugation between the two di-2-naphthyloxadiazole moieties in **5**. These naphthalene trimers exhibited photoluminescence (PL) in a solution and in a solid state. These PL data are listed in Table 2. Compounds **4** and **5** exhibited three emission maxima, which appeared to be a result of the emission from the building unit based on **1** and the extended π-electron system. The quantum yields of **4** and **5** in dichloromethane were measured relative to **1** ($\Phi_{PL} = 0.85$)[2]. The quantum yield of **5** was close to 1. On the other hand, the quantum yield of **4** was lower than the quantum yields of **5** and **1**. These results indicate that

Table 1
Melting points, color, and absorption maxima

Compound	Mp (°C)	Color	λ_{max} (log ε)[a] (nm)
4	282.5[b]	Colorless	341 sh (4.57), 321 (4.83), 277 (4.83), 227 (4.85)
5	358.7[b]	Pale yellow	361 sh, 343, 271, 228[c]
1	194–195	Colorless	339 sh (4.23), 317 (4.51), 267 (4.66), 233 (4.61)

[a] In CH_2Cl_2.
[b] Measured in DSC.
[c] The molar absorption coefficients were not obtained.

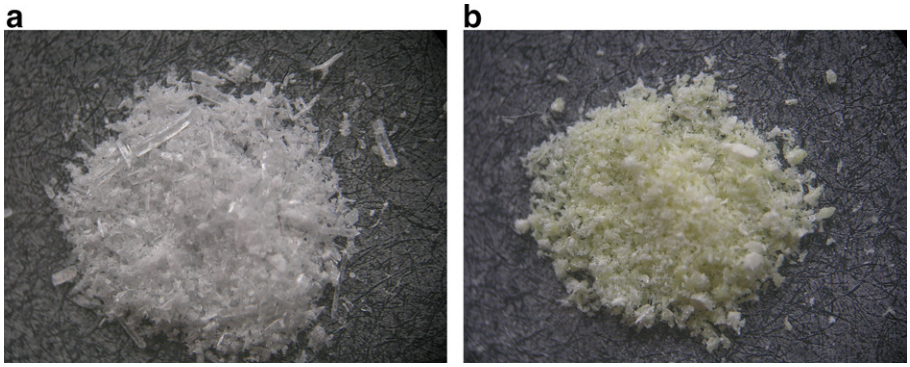

Figure 2. Color of the solids of **4** (a) and **5** (b).

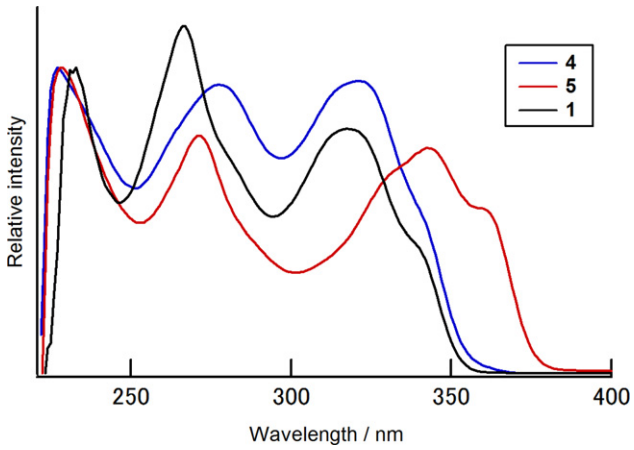

Figure 3. UV–vis absorption spectra.

Table 2
Emission maxima and quantum yields

Compound	λ_{em}[a] (nm)	$\lambda_{em,\ film}$ (nm)	Φ_{PL}[a,b]
4	400 sh, 385, 365	402	0.74 ± 0.02
5	420 sh, 394, 373	449, 426 sh	0.97 ± 0.02
1	392 sh, 370, 352	392 sh, 379	0.85

[a] In CH_2Cl_2.
[b] Measured relative to **1**, λ_{ex} = 317 nm.

the orientation between fluorophores affects the emissive characteristics. The fluorescence spectra of **4** and **5** in the solid state were measured, and their emission maxima are listed in Table 2. The maxima of **5** are red-shifted as compared to those in the solution state, although the maxima of **4** and **1** are similar to those in the solution state. This result was attributed to the strong intermolecular interactions of **5** in the solid state. The cyclic voltammetry (CV) of **4** in *N,N*-dimethylformamide (DMF) revealed a quasi-reversible reduction wave.[14] The reduction wave of **5** was not obtained because of its low solubility. The half-wave reduction potentials of **4** and **1** were observed to be −2.11 and −2.19 V versus Fc/Fc^+, respectively. The reduction potential of **4** was similar to that of **1**.

In order to estimate the influence of regioisomers on molecular orbitals, B3LYP/6-31G(d) calculations[15] of compounds **4** and **5** were performed using the coordinates obtained from X-ray crystallographic analyses. The energy of LUMO was lower in **5** than that in **4** (LUMO/eV: **4**, −1.92; **5**, −2.10). This result indicated that the π-conjugation between electron-accepting moieties affected their LUMO energy levels. The energy of HOMO was higher in **5** than that in **4** (HOMO/eV: **4**, −5.94; **5**, −5.77). Therefore, the HOMO–LUMO energy gap of **5** was smaller than that of **4** (gap/eV: **4**, 4.02; **5**, 3.67). The result is consistent with that of the respective absorption edges.

The molecular structures of **4** and **5** were investigated by X-ray crystallographic analyses.[16] Single crystals of **4** and **5** were grown by sublimation. In the crystal, the molecular structure of **4** was almost planar and W-shaped (Fig. 4a). The dihedral angle between the oxadiazole rings and the terminal naphthalene groups was 3.85°. Compound **4** crystallized in the monoclinic *C*2/*c*. The molecules were stacked along the *a* axis to form a column with

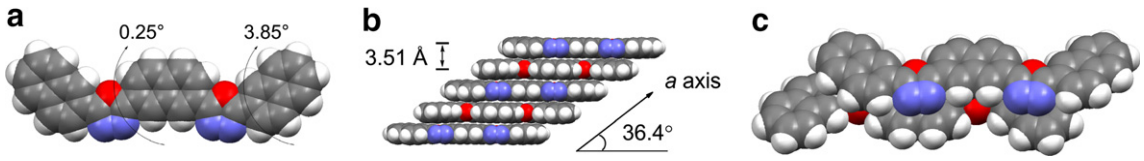

Figure 4. Crystal structure of **4**: (a) molecular structure; (b) crystal packing; (c) overlap mode.

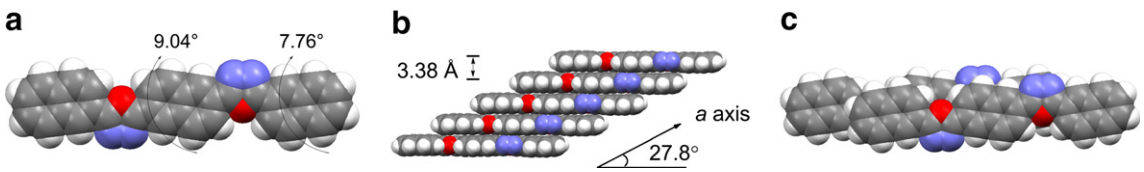

Figure 5. Crystal structure of **5**: (a) molecular structure; (b) crystal packing; (c) overlap mode.

an intermolecular distance of 3.51 Å (Fig. 4b). This value is slightly longer than the sum of the van der Waals radii of carbon atoms (C···C = 3.40 Å). The molecular stacking was induced by electrostatic intermolecular interactions between the 1,3,4-oxadiazole rings and the naphthalene moieties (Fig. 4c). The W-shaped molecular structure was preferred over the dense crystal packing. The molecular structure of **5** was also almost planar and linear (Fig. 5a). The dihedral angle between the oxadiazole rings and the central naphthalene moiety was 9.04°. Compound **5** crystallized in the monoclinic $P2_1/c$. The molecules were stacked along the *a* axis to form a column with an intermolecular distance of 3.38 Å (Fig. 5b). This value was slightly shorter than the sum of the van der Waals radii of carbon atoms. The strong molecular overlap is attributed to the electrostatic π···π interactions between the 1,3,4-oxadiazole rings and the naphthalene moieties (Fig. 5c). The calculated density of **5** was higher than that of **4** (D_c/g cm^{-3}: **4**, 1.390; **5**, 1.437).

In summary, we synthesized two regioisomers of naphthalene trimers linked by 1,3,4-oxadiazole spacers (**4** and **5**). Compounds **4** and **5** were obtained in the forms of colorless crystals and pale yellow solids, respectively. The melting point of **5** was higher than that of **4**. The X-ray crystallographic analysis of **5** revealed a π-stacked column with a shorter intermolecular distance than the sum of the van der Waals radii of carbon atoms. The absorption maximum of **5** in dichloromethane was red-shifted as compared to that of **4**, indicating the π-conjugation between the two di-2-naphthyloxadiazole moieties in **5**. The quantum yields of **4** and **5** were measured to be 0.74 and 0.97 relative to that of **1** (0.85). Furthermore, **5** has a higher electron affinity than **4**. These results were supported by the HOMO and LUMO energies of **4** and **5** obtained from the MO calculations. These results revealed that the crosslinking of building blocks is important for the design of functional materials. Because these compounds are candidates for applications, such as electron-transporting materials in EL devices, a further investigation of their potential applications is in progress.

Acknowledgments

This work was supported by a Grant-in-Aid for Scientific Research (No. 19550034) from the Ministry of Education, Culture, Sports, Science and Technology, Japan. The authors thank the Instrument Center of the Institute for Molecular Science for the crystal analyses.

References and notes

1. Hughes, G.; Bryce, M. R. *J. Mater. Chem.* **2005**, *15*, 94–107.
2. Nijegorodov, N. I.; Downey, W. S. *Spectrochim. Acta, Part A* **1995**, *51*, 2335–2346.
3. (a) Yeh, H.-C.; Lee, R.-H.; Chan, L.-H.; Lin, T.-Y. J.; Chen, C.-T.; Balasubramaniam, E.; Tao, Y.-T. *Chem. Mater.* **2001**, *13*, 2788–2796; (b) Tamoto, N.; Adachi, C.; Nagai, K. *Chem. Mater.* **1997**, *9*, 1077–1085.
4. Adachi, C.; Tsutsui, T.; Saito, S. *Appl. Phys. Lett.* **1989**, *55*, 1489–1491.
5. (a) Salbeck, J.; Yu, N.; Bauer, J.; Weissörtel, F.; Bestgen, H. *Synth. Met.* **1997**, *91*, 209–215; (b) Salbeck, J.; Weissörtel, F. *Macromol. Symp.* **1997**, *125*, 121–132; (c) Johansson, N.; dos Santos, D. A.; Guo, S.; Cornil, J.; Fahlman, M.; Salbeck, J.; Schenk, H.; Arwin, H.; Brédas, J. L.; Salanek, W. R. *J. Chem. Phys.* **1997**, *107*, 2542–2549.
6. (a) Bettenhausen, J.; Strohriegl, P. *Adv. Mater.* **1996**, *8*, 507–510; (b) Bettenhausen, J.; Greczmiel, M.; Jandke, M.; Strohriegl, P. *Synth. Met.* **1997**, *91*, 223–228; (c) Bettenhausen, J.; Strohriegl, P. *Macromol. Rapid Commun.* **1996**, *17*, 623–631; (d) Tokito, S.; Tanaka, H.; Noda, K.; Okada, A.; Taga, Y. *Macromol. Symp.* **1997**, *125*, 181–188; (e) Naito, K.; Sakurai, M.; Egusa, S. *J. Phys. Chem. A* **1997**, *101*, 2350–2357.
7. Ono, K.; Ezaka, S.; Higashibata, A.; Hosokawa, R.; Ohkita, M.; Saito, K.; Suto, M.; Tomura, M.; Matsushita, Y.; Naka, S.; Okada, H.; Onnagawa, H. *Macromol. Chem. Phys.* **2005**, *206*, 1576–1582.
8. Zafiropoulos, N. A.; Choi, E-J.; Dingemans, T.; Lin, W.; Samulski, E. T. *Chem. Mater.* **2008**, *20*, 3821–3831.
9. ^{1}H NMR for **7a**–**b**. Compound **7a**: ^{1}H NMR (DMSO-d_6): δ 4.59 (br s, 4H), 7.99 (d, *J* = 8.5 Hz, 2H), 8.04 (d, *J* = 8.5 Hz, 2H), 8.48 (s, 2H), 10.00 (br s, 2H). Compound **7b**: ^{1}H NMR (DMSO-d_6): δ 4.60 (br s, 4H), 7.96 (d, *J* = 8.9 Hz, 2H), 8.08 (d, *J* = 8.9 Hz, 2H), 8.46 (s, 2H), 10.01 (br s, 2H).
10. ^{1}H NMR for **8a**–**b**. Compound **8a**: ^{1}H NMR (DMSO-d_6): δ 7.64–7.70 (m, 4H), 8.02–8.22 (m, 12H), 8.61 (s, 2H), 8.72 (s, 2H), 10.80 (s, 2H), 10.87 (s, 2H). Compound **8b**: ^{1}H NMR (DMSO-d_6): δ 7.66–7.68 (m, 4H), 8.05–8.13 (m, 10H), 8.26 (d, *J* = 8.5 Hz, 2H), 8.61 (s, 2H), 8.67 (s, 2H), 10.80 (s, 2H), 10.85 (s, 2H).
11. Data for **4**. 39% yield. Mp 288–289 °C. ^{1}H NMR ($CDCl_3$): δ 7.62–7.65 (m, 4H), 7.93–7.97 (m, 2H), 8.03–8.07 (m, 4H), 8.11 (d, *J* = 8.6 Hz, 2H), 8.29 (dd, *J* = 8.6, 1.6 Hz, 2H), 8.41 (d, *J* = 8.6 Hz, 2H), 8.72 (s, 2H), 8.86 (s, 2H). IR (KBr): 3052, 1555, 1539, 1495, 1186, 1069, 847, 754, 469 cm^{-1}. Mass: *m*/*z* (%) 516 (100) [M$^+$], 347 (37), 155 (68), 127 (42). Anal. Calcd for $C_{34}H_{20}N_4O_2$: C, 79.06; H, 3.90; N, 10.85. Found: C, 78.97; H, 3.80; N, 10.86.
12. Data for **5**. 44% yield. Mp >300 °C. IR (KBr): 3050, 1553, 1485, 1364, 1182, 1069, 968, 905, 872, 822, 756, 473 cm^{-1}. Mass: *m*/*z* (%) 516 (100) [M$^+$], 155 (92), 127 (65). Anal. Calcd for $C_{34}H_{20}N_4O_2$: C, 79.06; H, 3.90; N, 10.85. Found: C, 79.13; H, 3.81; N, 10.93.
13. The DSC measurements of **4** and **5** were carried out at an increasing temperature rate of 10 °C min^{-1} under nitrogen.
14. The CV measurement of **4** was performed in DMF with 0.1 M *n*-Bu_4NClO_4 at a scanning rate of 500 mV s^{-1} using Pt and Ag/Ag$^+$ electrodes. The value is expressed in a potential versus Fc/Fc$^+$.
15. Frisch, M. J.; Trucks, G. W.; Schlegel, H. B.; Scuseria, G. E.; Robb, M. A.; Cheeseman, J. R.; Montgomery, J. A., Jr.; Vreven, T.; Kudin, K. N.; Burant, J. C.; Millam, J. M.; Iyengar, S. S.; Tomasi, J.; Barone, V.; Mennucci, B.; Cossi, M.; Scalmani, G.; Rega, N.; Petersson, G. A.; Nakatsuji, H.; Hada, M.; Ehara, M.; Toyota, K.; Fukuda, R.; Hasegawa, J.; Ishida, M.; Nakajima, T.; Honda, Y.; Kitao, O.; Nakai, H.; Klene, M.; Li, X.; Knox, J. E.; Hratchian, H. P.; Cross, J. B.; Adamo, C.; Jaramillo, J.; Gomperts, R.; Stratmann, R. E.; Yazyev, O.; Austin, A. J.; Cammi, R.; Pomelli, C.; Ochterski, J. W.; Ayala, P. Y.; Morokuma, K.; Voth, G. A.; Salvador, P.; Dannenberg, J. J.; Zakrzewski, V. G.; Dapprich, S.; Daniels, A. D.; Strain, M. C.; Farkas, O.; Malick, D. K.; Rabuck, A. D.; Raghavachari, K.; Foresman, J. B.; Ortiz, J. V.; Cui, Q.; Baboul, A. G.; Clifford, S.; Cioslowski, J.; Stefanov, B. B.; Liu, G.; Liashenko, A.; Piskorz, P.; Komaromi, I.; Martin, R. L.; Fox, D. J.; Keith, T.; Al-Laham, M. A.; Peng, C. Y.; Nanayakkara, A.; Challacombe, M.; Gill, P. M. W.; Johnson, B.; Chen, W.; Wong, M. W.; Gonzalez, C.; Pople, J. A. GAUSSIAN 03: *Revision C.02*; Gaussian: Wallingford, CT, 2004.
16. Crystal data for **4**: colorless block, 0.30 × 0.25 × 0.15 mm, $C_{34}H_{20}N_4O_2$, *M* = 516.55, monoclinic, space group *C*2/*c*, *a* = 17.977(5), *b* = 13.110(3), *c* = 11.765(3) Å, *β* = 117.070(5)°, *V* = 2468(1) Å^3, *Z* = 4, D_c = 1.390 g cm^{-3}, *μ* = 0.88 cm^{-1}, *F*(000) = 1072, *T* = 296 K, 2774 unique reflections [$I > 2\sigma(I)$], R_1 = 0.1090, R_w = 0.2494, GOF = 2.393. CCDC 686868.
Crystal data for **5**: colorless block, 0.15 × 0.08 × 0.03 mm, $C_{34}H_{20}N_4O_2$, *M* = 516.55, monoclinic, space group $P2_1/c$, *a* = 7.180(3), *b* = 14.840(5), *c* = 11.750(5) Å, *β* = 107.578(2)°, *V* = 1193.4(8) Å^3, *Z* = 2, D_c = 1.437 g cm^{-3}, *μ* = 0.92 cm^{-1}, *F*(000) = 536, *T* = 173 K, 2730 unique reflections [$I > 2\sigma(I)$], R_1 = 0.0767, R_w = 0.1726, GOF = 1.128. CCDC 686869.